



RESEARCH PAPER

RIN13-mediated disease resistance depends on the SNC1–EDS1/PAD4 signaling pathway in Arabidopsis

Xiaoxiao Liu¹, Hui Liu¹, Jingjing He¹, Siyuan Zhang¹, Hui Han¹, Zhangying Wang¹, Wen-Cheng Liu², Yun-Kuan Liang^{1,*} and Zhiyong Gao^{1,*} 

¹ State Key Laboratory of Hybrid Rice, Key Laboratory for Research and Utilization of Heterosis in Indica Rice of Ministry of Agriculture, College of Life Sciences, Wuhan University, Wuhan 430072, China

² State Key Laboratory of Cotton Biology, State Key Laboratory of Crop Stress Adaptation and Improvement, School of Life Sciences, Henan University, Kaifeng 475004, China

* Correspondence: zygao@whu.edu.cn or ykliang@whu.edu.cn

Received 13 May 2020; Editorial decision 2 September 2020; Accepted 14 September 2020

Editor: Jacqueline Monaghan, Queen's University, Canada

Abstract

Plants have evolved an innate immune system to protect themselves from pathogen invasion with the help of intracellular nucleotide-binding leucine-rich repeat (NLR) receptors, though the mechanisms remain largely undefined. RIN13 (RPM1-interacting protein 13) was previously reported to enhance disease resistance, and suppress RPM1 (a CNL-type NLR)-mediated hypersensitive response in Arabidopsis via an as yet unknown mechanism. Here, we show that RIN13 is a nuclear-localized protein, and functions therein. Overexpression of RIN13 leads to autoimmunity with high accumulation of salicylic acid (SA), constitutive expression of pathogenesis-related genes, enhanced resistance to a virulent pathogen, and dwarfism. In addition, genetic and transcriptome analyses show that SA-dependent and SA-independent pathways are both required for RIN13-mediated disease resistance, with the EDS1/PAD4 complex as an integration point. RIN13-induced dwarfism was rescued completely by either the *pad4-1* or the *eds1-2* mutant but partially by *snc1-r1*, a mutant of the TNL gene *SNC1*, suggesting the involvement of EDS1/PAD4 and SNC1 in RIN13 functioning. Furthermore, transient expression assays indicated that RIN13 promotes the nuclear accumulation of PAD4. Collectively, our study uncovered a signaling pathway whereby SNC1 and EDS1/PAD4 act together to modulate RIN13-triggered plant defense responses.

Keywords: Arabidopsis, disease resistance, EDS1, NLR, PAD4, RIN13, salicylic acid.

Introduction

Plants protect themselves against destructive pathogens and pests using a two-layered innate immune system: pathogen-associated molecular pattern (PAMP)-triggered immunity (PTI) and effector-triggered immunity (ETI) (Jones and Dangl, 2006). Pattern recognition receptors (PRRs) can recognize the highly conserved PAMPs to stimulate an immune response, named PTI (Couto and Zipfel, 2016; Tang *et al.*, 2017). To enhance pathogenicity, pathogens have

evolved virulence proteins ('effectors') to suppress PTI. In response, plants have adapted by obtaining multiple intracellular nucleotide-binding leucine-rich repeat [NB-LRR (NLR)] receptors to detect effectors, and stimulate ETI. Thus, while pathogen effectors are collectively required for disease, any single effector can be potentially recognized by a plant with a corresponding NLR receptor. Activation of the NLR proteins leads to stronger and faster immune responses

than PTI, and usually results in programmed cell death (PCD) which is named the hypersensitive response (HR) (Dodds and Rathjen, 2010; Cui *et al.*, 2015). In Arabidopsis, there are ~150 NLR proteins that can be divided into two categories on the basis of the presence of an N-terminal domain: Toll-like/Interleukin 1 receptor (TIR)-type NLR (TNL) proteins and coiled-coil (CC)-type NLR (CNL) proteins (Cui *et al.*, 2015; Jones *et al.*, 2016).

ETI not only suppresses pathogen invasion at infection sites, but also generates mobile signals to induce systemic acquired resistance (SAR) to protect the rest of the plant from secondary infection (Fu and Dong, 2013). The plant hormone salicylic acid (SA) is required for SAR establishment (Gaffney *et al.*, 1993). Over 90% of SA is synthesized through the isochorismate synthase 1 (ICS1)-mediated pathway (Yang *et al.*, 2015; Rekhter *et al.*, 2019). Nonexpresser of PR genes 1 (NPR1) and its paralogs NPR3 and NPR4 are SA receptors that mediate SA-induced immune responses (Kinkema *et al.*, 2000; Fu *et al.*, 2012; Ding *et al.*, 2018). SA induces the expression of PR genes such as PR1, PR2, and PR5 to confer broad spectrum resistance (Uknes *et al.*, 1992).

The lipase-like Phytoalexin Deficient 4 (PAD4) has been found to be required for SA signaling, and to interact directly with Enhanced Disease Susceptibility 1 (EDS1) to form a heterodimer complex to regulate plant immunity (Feys *et al.*, 2001). Disease resistance conferred by TNL proteins depends on either the EDS1/PAD4 or the EDS1/SAG101 complex (Feys *et al.*, 2001; Shirano *et al.*, 2002; Zhang *et al.*, 2003; Wirthmueller *et al.*, 2007). EDS1 and PAD4 promote the accumulation of SA which in turn up-regulates the expression of EDS1 and PAD4, thus forming a positive feedback to augment SA-triggered immune responses (Zhou *et al.*, 1998; Jirage *et al.*, 1999; Feys *et al.*, 2001; Vlot *et al.*, 2009). EDS1 and PAD4 also participate in SA-independent pathways to induce defense gene expression and pathogen resistance (Cui *et al.*, 2017, 2018). It is of note that, although EDS1 and PAD4 often work as a complex, they can also function independently. For example, apart from PAD4, EDS1 interacts with SAG101 to mediate TNL-induced cell death through the EDS1-SAG101-NRG1 module (Wagner *et al.*, 2013; Lapin *et al.*, 2019), whereas PAD4 mediates the resistance to green peach aphid in an EDS1-independent way (Pegadaraju *et al.*, 2007; Dongus *et al.*, 2020). EDS1 and PAD4 play essential roles in plant physiology and immune responses, although knowledge of their mechanism remains fragmentary.

RIN13 has been demonstrated to interact with the NB-ARC domain of RPM1, a model CNL protein for the study of ETI. Ectopic expression of RIN13 under the control of the *Cauliflower mosaic virus* (CaMV) 35S promoter (hereafter 35S) in Arabidopsis could efficiently abolish RPM1-mediated HR while enhancing disease resistance (Al-Daoude *et al.*, 2005). However, the mechanism of RIN13 action has not been elucidated. RIN13 is composed of 430 amino acids, and does not have any discernible motifs. We generated stable 35S::RIN13-YFP-HA transgenic plants to investigate RIN13 at the protein level. We found that RIN13 functions in the nucleus, and overexpression of RIN13 induces autoimmunity with high accumulation of SA, constitutive

expression of PR genes, enhanced resistance to the virulent pathogen *Pseudomonas syringae* pathovar *tomato* (Pst) DC3000, and dwarfism in plants. Importantly, the RIN13-induced dwarf phenotype is EDS1/PAD4 dependent but SA independent, and knocking out the TNL gene *SNC1*, but not the CNL gene *RPM1*, partially rescued the dwarf phenotype. Our study revealed a novel signaling pathway that employs the EDS1/PAD4 complex for RIN13 promoting plant defense through the TNL class of NLR receptors.

Materials and methods

Plant materials and growth conditions

All Arabidopsis (*Arabidopsis thaliana* L.) and *Nicotiana benthamiana* plants were grown in pots with autoclaved vermiculite. Hoagland solution was regularly added to supply nutrients for plant growth. Arabidopsis plants for bacterial growth assays were grown in a controlled-environment chamber at 22 °C under an 8 h/16 h light/dark cycle with relative humidity at 65±10%. Plants for setting seeds or genetic transformation were grown under a 16 h/8 h light/dark cycle with relative humidity at 65±10%. For plants grown in sterile conditions, sterilized seeds were sown in autoclaved 480 ml (diameter, 90 mm; height, 110 mm) plant tissue culture bottles filled with a half volume of vermiculite. Filter-sterilized Hoagland solution was supplied twice in 6 weeks.

Arabidopsis mutant lines *pad4-1* (Jirage *et al.*, 1999) and *snc1-r1* (Zhang *et al.*, 2003) were kindly provided by Dr Wei Xiao (University of Saskatchewan) and Dr Xin Li (University of British Columbia); *eds1-2* (Falk *et al.*, 1999) by Dr Haitao Cui (Fujian Agriculture and Forestry University); *sid2-2* (Wildermuth *et al.*, 2001; Chen *et al.*, 2009; Yuan *et al.*, 2017) by Dr Ying-Tang Lu (Wuhan University); *npr1-1* (Cao *et al.*, 1997) by Dr Guoyong Xu (Wuhan University); and *rpm1-3* (Grant *et al.*, 1995) by Dr Jeffery L. Dangl (University of North Carolina at Chapel Hill). The *rin13* mutant (SALK_001145) was ordered from the Arabidopsis Biological Resource Center (ABRC). All Arabidopsis used in this study are in the Col-0 background. All primers used in this study are listed in Supplementary Table S1 at JXB online.

Vector constructions and transgenic lines

The coding sequences (CDS) of RIN13, PAD4, and EDS1 from Arabidopsis were cloned into an entry vector pENTR/D-TOPO (Thermo Fisher Scientific), and were subsequently introduced into the destination vector pEarleyGate 101 (Karimi *et al.*, 2002) with LR clonase (Thermo Fisher Scientific) to obtain 35S::RIN13-YFP-HA, 35S::PAD4-YFP-HA, and 35S::EDS1-YFP-HA constructs. The T7 tag sequence was fused to the 5' cDNA sequence of RIN13 to obtain T7-RIN13. T7-RIN13 and RIN13 were cloned into the pEarleyGate 100 vector (Karimi *et al.*, 2002) to obtain 35S::T7-RIN13 and 35S::RIN13 constructs. The NES (nuclear export signal) or its negative control nes sequence (Gao *et al.*, 2011) was fused to the 3' DNA sequence of HA in pEarleyGate 101, and RIN13 was cloned into the modified vectors to obtain 35S::RIN13-YFP-HA-NES and 35S::RIN13-YFP-HA-nes constructs. 35S::RIN13-YFP-HA, 35S::RIN13-YFP-HA-NES, 35S::RIN13-YFP-HA-nes, 35S::T7-RIN13, and 35S::RIN13 constructs were each transformed into Col-0, to obtain stable transgenic plants with the floral dipping method (Clough and Bent, 1998). Over 20 independent transgenic lines were collected for each transgenic material.

Transient protein expression system

Transient protein expression in *N. benthamiana* was performed as previously described (Yuan *et al.*, 2018). In brief, overnight-cultivated agrobacteria (GV3101) were suspended in MES buffer and incubated at room temperature for 1 h. Agrobacteria were infiltrated into the leaves of *N. benthamiana* at the desired OD₆₀₀ values together with agrobacteria expressing P19 at a final OD₆₀₀ of 0.2.

Trypan blue staining

The leaves of *N. benthamiana* transiently expressing proteins were collected at day 5 post-infiltration, and then incubated with trypan blue stain solution (250 g of phenol crystals, 250 ml of glycerol, 250 ml of lactic acid, 0.5 g of trypan blue, 250 ml of ddH₂O) in 50 ml blue cap tubes (Thermo Fisher Scientific). The leaves were heated in boiling solution for 5 min, and stained at room temperature for 30 min. The stained leaves were rinsed with chloral hydrate solution (250 g of chloral hydrate, 100 ml of H₂O) to clear the background. Three replicates were conducted for the stainings.

Protein extraction and detection

Total proteins from leaves of *Arabidopsis* or *N. benthamiana* were extracted with extraction buffer (20 mM Tris–HCl pH 8.0, 5 mM EDTA, 10 mM DTT, 1% SDS). Nuclear proteins were extracted as described by Ding *et al.*, 2012. Extracted proteins were separated on SDS–PAGE gels, and transferred to nitrocellulose membranes. Target proteins were detected with antibodies. The primary antibodies are anti-HA (Roche, #11867423001), anti-T7 (EMD Millipore, #69522), anti- β -actin (Abbkine, #A01050-2), and anti-histone H3 (Abcam, #ab1791). At least three replicates were performed for each detection.

Confocal microscopy

Leaves of *Arabidopsis* and *N. benthamiana* plants were infiltrated with 10 μ g ml⁻¹ 4',6-diamidino-2-phenylindole (DAPI) staining for 20 min before microscopic observation. Leaves were cut into ~10 mm² leaf strips; the abaxial surface of the sample was observed on the slide with a confocal microscope (FV10-ASW, Olympus). Yellow fluorescent protein (YFP) and DAPI fluorescence were excited at 488 nm and 405 nm, respectively. Three replicates and >50 cells with similar subcellular locations were examined.

Bacterial growth assay

Pst DC3000 (*avrB*) or *Pst* DC3000 [2.5 \times 10⁷ colony-forming units (CFU) ml⁻¹, with 0.02% Silwet L-77] was sprayed on the leaf surface of 4-week-old plants. The inoculated plants were covered with a dome for 2 d. Samples were collected at 1 h and 72 h post-inoculation. Five to six leaves were put into a 1.5 ml tube containing 1 ml of 10 mM MgCl₂ with 0.02% Silwet L-77, and gently shaken at 30 °C for 1 h at 250 rpm. The solution was diluted in series, and the numbers of bacterial colonies on the plates were counted (Tornero and Dangl, 2001). The experiment was repeated three times with four technique replicates for each assay.

RNA extraction, RNA-sequencing, and qRT–PCR analysis

A 2 g aliquot of 4-week-old *Arabidopsis* leaves frozen in liquid nitrogen was ground to a fine powder. Total RNA was extracted with an RNAprep Pure Plant Kit (Tiangen Biotech, DP432). mRNA was separated by oligo(dT) magnetic beads for constructing the cDNA library. Illumina HiSeq™2000 was used to perform the sequencing to obtain the raw reads, which subsequently were filtered by cutadapter (version 1.11) to remove adapter sequences and low quality reads. The remaining reads were quality checked by fastqc (version: 0.11.5) (<http://www.bioinformatics.babraham.ac.uk/projects/fastqc/>) to generate ~40 million clean reads (6 G of clean data) per sample. The clean reads were mapped to the *Arabidopsis* genome (ftp://ftp.ensemblgenomes.org/pub/plants/release-39/fasta/arabidopsis_thaliana/) using Hisat2 (Kim *et al.*, 2015). The edgeR program (Robinson *et al.*, 2010) was used to perform the differential expression analysis. Genes with a false discovery rate (FDR) <0.05 and |log₂ (fold change)|>1 were considered to be the differentially significant genes. RNA-sequencing was performed by IGENEBOOK Biotechnology Ltd (Wuhan). Three biological replicates were conducted for each assay.

Quantitative reverse transcription–PCR (qRT–PCR) was performed as previously described (Li *et al.*, 2019). The transcriptional level of

ACTIN 2 was used as an internal control. All primers used for qRT–PCR are listed in Supplementary Table S2.

Plant hormone analysis

The quantification of plant hormones was performed as previously described with slight modifications (Dobrev and Vankova, 2012). In brief, 100 mg of plant leaves were ground, and the powder was extracted with 1 ml of methanol containing 20% water at 4 °C for 12 h. The extract was centrifuged at 12 000 g at 4 °C for 15 min. The supernatant was collected and evaporated to dryness under a nitrogen gas stream, and reconstituted in 100 ml of acetonitrile containing 5% water. The solution was centrifuged, and the supernatant was collected for analysis using an LC–ESI–MS/MS system (HPLC, Shim-pack UFLC SHIMADZU CBM30A system; MS, Applied Biosystems 4500 Q TRAP). Similar results were obtained in triplicate experiments under the same conditions. The experiments were performed by Wuhan Metware Biotechnology Co., Ltd (Wuhan).

Quantitative analysis of the YFP fluorescence

EDS1–YFP–HA or PAD4–YFP–HA were transiently expressed with and without T7–RIN13 in the leaves of *N. benthamiana*. Fluorescence images were photographed by a Zeiss Axio Imager M2 at identical settings. The YFP fluorescence intensity in the nucleus was evaluated with the Zeiss ZEN software. Over 30 nuclei were measured for each sample.

Yeast two-hybrid system

The CDS of *RIN13* was cloned into pGBKT7 and pGADT7. Then, the vectors were transformed into gold yeast to test self-activation according to instructions from the manufacturer (Clontech, Japan). DDO, double dropout (SD/–Leu/–Trp); QDO/X, quadruple dropout (SD/–Ade/–His/–Leu/–Trp with X– α -Gal).

Statistical analysis

Data processing and analysis were performed using SIGMAPLOT 10 (Systat Software Inc., San Jose, CA, USA). Significant differences were determined by Student's *t*-test, and marked in the figures as ****P*<0.001, ***P*<0.01, and **P*<0.05. A non-significant difference was marked as ns.

Results

Overexpression of RIN13 leads to dwarfism

To evaluate the function of RIN13 at the protein level, the expression construct of *p35S::RIN13-YFP-HA* was made, and then transformed into wild-type (WT) *Arabidopsis* to generate stable transgenic plants. We had a quick look at the first 20 resultant transgenic plants that survived from the transgene selection. Eight plants displayed pronounced dwarfism which is accompanied by leaf senescence, though at varying levels. Of note, the dwarf and senescent phenotypes started to appear when the transgenic seedlings reached 3 weeks of age, and became most pronounced at 6 weeks old (Supplementary Fig. S1). Importantly, these eight plants overall had a higher protein abundance of RIN13 than the remaining 12 transformants. Furthermore, we found that the severity of the dwarf phenotype was positively correlated with the protein levels of RIN13–YFP–HA (Fig. 1A, B). We also generated N-terminal tagged *T7-RIN13* and non-tagged *RIN13* transgenic plants to preclude the influence of tags (Fig. 1C, D). Both N-terminal tagged *T7-RIN13* and non-tagged *RIN13* transgenic plants

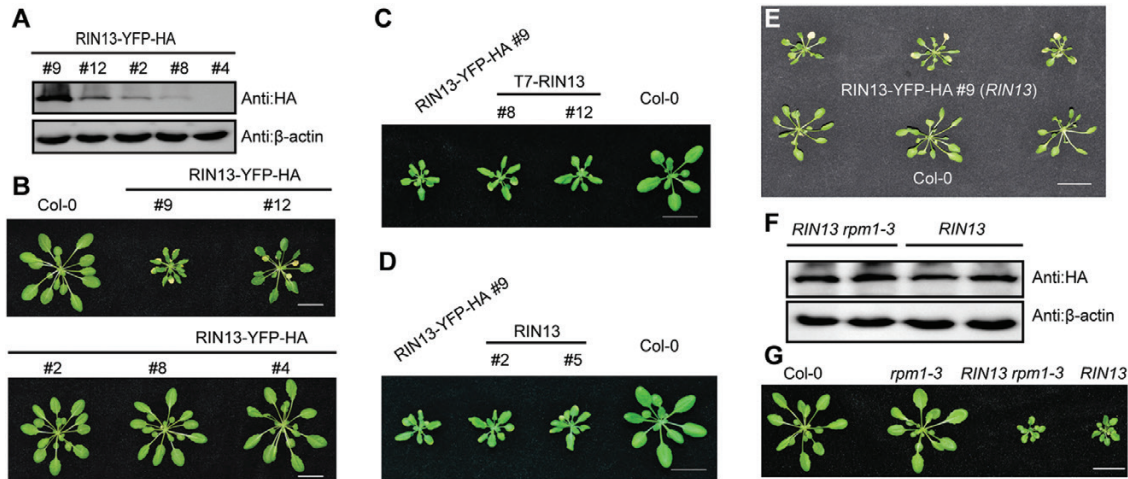


Fig. 1. Overexpression of *RIN13* induces a dwarf phenotype. (A) Protein levels of RIN13–YFP–HA in stable transgenic lines. The protein level of RIN13 was detected with anti-HA antibody. β -Actin was used as a protein loading control. The lines were arranged according to the level of RIN13–YFP–HA accumulation in the transgenic lines. (B) The phenotypes of the 6-week-old transgenic plants and Col-0. The phenotypes of 4-week-old *T7-RIN13* (C) and non-tagged *RIN13* (D) transgenic lines. (E) The phenotypes of the 6-week-old transgenic plants (line #9) and Col-0 grown under sterile conditions. (F) The protein levels of RIN13–YFP–HA in *RIN13 rpm1-3* and *RIN13* plants. (G) *rpm1-3* does not restore the dwarf phenotype of *RIN13*. Five-week-old plants were photographed. Plants in (B), (E), and (G) were grown under an 8 h/16 h light/dark cycle, and plants in (C) and (D) were grown under a 16 h light/8 h dark photoperiod. Scale bar=2 cm. (This figure is available in color at *JXB* online.)

show the dwarf phenotype, indicating that neither the N-terminal T7 tag nor the C-terminal YFP–HA tag affects the overexpression phenotype of *RIN13*, and the dwarf phenotype is indeed caused by the accumulation of *RIN13* protein over a certain threshold. Given that all eight transgenic plants (each is an independent line) presented the same kind of phenotype, we therefore decided to concentrate our efforts on one of the most discernible, namely #9 (*RIN13-YFP-HA*), as shown in Fig. 1B (hereafter referred to as *RIN13* for brevity) for further investigation.

We cultivated the plants in sterile bottles to preclude any potential effects of biotic stresses from the plant growth facilities. *RIN13* plants consistently showed a dwarf phenotype in sterile conditions, while WT plants (Col-0) grew perfectly healthily (Fig. 1E), indicating that the phenotype is not caused by unknown environmental factors. Furthermore, we crossed *RIN13* with *rpm1-3*, a loss-of-function mutant of *RPM1* (Grant et al., 1995), to generate *RIN13 rpm1-3* plants which displayed the characteristic dwarf phenotype similar to that of *RIN13*, suggesting that the dwarf phenotype triggered by overexpression of *RIN13* is independent of *RPM1* (Fig. 1F, G).

RIN13 functions in the nucleus

Our previous results indicated that *RIN13* is localized in the nucleus when transiently expressed in *N. benthamiana* (Liu et al., 2020). To further confirm this result in Arabidopsis, we examined its subcellular localization in *RIN13* plants by confocal microscopy. The data shown in Fig. 2A indicated that *RIN13* is a nuclear-localized protein. Next, the nuclear location of *RIN13* was verified biochemically. The same nuclear location of *RIN13* was observed in Arabidopsis with *RIN13-YFP-HA* and *T7-RIN13* stably expressed lines, respectively (Fig. 2B).

To determine whether the nuclear location of *RIN13* is essential for its function, we fused an NES to the C-terminus of *RIN13-YFP-HA* to drive *RIN13* out of the nucleus and, at the same time, we fused nes to the C-terminus of *RIN13-YFP-HA* as an experimental control. Stable *35S::RIN13-YFP-HA-NES* or *35S::RIN13-YFP-HA-nes* transgenic lines were generated, and two independent lines with similar protein levels of *RIN13* were selected for the subsequent research (Fig. 2C). As shown in Fig. 2D, the NES could efficiently drive *RIN13-YFP-HA* out of the nucleus. As expected, *RIN13-YFP-HA-NES* plants lost the dwarf phenotype whereas *RIN13-YFP-HA-nes* plants did not (Fig. 2E). These observations firmly established *RIN13* as a nuclear-localized regulator. In line with this, *RIN13-YFP-HA-NES* was unable to induce cell death when expressed in the leaves of *N. benthamiana* (Supplementary Fig. S2).

It is worth mentioning that Arabidopsis cells express a *RIN13*-related protein, At4g28690, which shares 32% identity with *RIN13* (Al-Daoude et al., 2005), and was therefore named *RIN13-Like* (*RIN13-L*). *RIN13-L* is also localized in the nucleus, and can induce cell death when transiently expressed in *N. benthamiana* (Supplementary Fig. S3).

Overexpression of *RIN13* leads to autoimmunity

We challenged *RIN13* transgenic plants with *Pst* DC3000 (*avrB*) to determine whether *RIN13* enhances *RPM1*-mediated resistance. Both *RIN13* transgenic plants and Col-0 suppressed the growth of the bacteria compared with the loss-of-function mutant *rpm1-3*, and *RIN13* plants showed stronger resistance than Col-0 (Fig. 3A), in accordance with the previous study by Al-Daoude et al. (2005). We also determined the disease resistance of *RIN13* to the virulent pathogen *Pst* DC3000. When *Pst* DC3000 was inoculated by spraying onto the surface of the leaves, *RIN13*

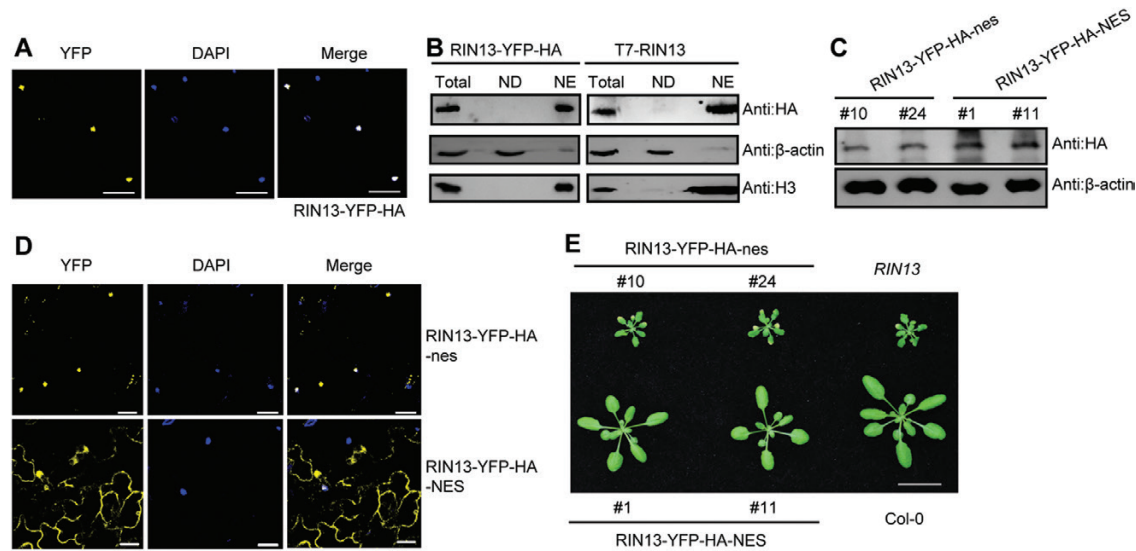


Fig. 2. RIN13 is localized in the nucleus, and functions therein. (A) Confocal images of RIN13–YFP–HA in the leaves of *RIN13* transgenic plants (*RIN13*). The location of RIN13–YFP–HA was observed by YFP fluorescence. Nuclei were visualized with DAPI staining. Scale bar=20 μ m. (B) RIN13 was detected in the nuclear fraction. Total proteins (Total) from transgenic plants were separated into a nuclear-depleted fraction (ND) and a nuclear-enriched fraction (NE). The distributions of RIN13–YFP–HA and T7-RIN13 were detected with an anti-HA antibody or anti-T7 antibody. β -Actin and histone H3 were used as internal references for ND and NE proteins, respectively. (C) Protein levels of RIN13–YFP–HA–NES and RIN13–YFP–HA–nes in stable transgenic plants. (D) Confocal images of RIN13–YFP–HA–NES and RIN13–YFP–HA–nes in Arabidopsis. Scale bar=20 μ m. (E) Phenotypes of *35S::RIN13-YFP-HA-NES* and *35S::RIN13-YFP-HA-nes* transgenic plants. Four-week-old plants grown under a 16 h/8 h light/dark cycle were photographed. Scale bar=2 cm. (This figure is available in color at *JXB* online.)

plants also exhibited stronger resistance to the pathogen compared with Col-0 and *rin13*, a loss-of-function mutant of RIN13 (Fig. 3B).

To gain further insights into the resistance mechanism of RIN13, we performed RNA-sequencing analysis to compare the genomic transcription between the 4-week-old *RIN13* and Col-0 plants. A total of 2750 and 2785 genes were up-regulated and down-regulated in *RIN13* plants, respectively (Fig. 3C). For the up-regulated genes, the top five enriched Gene Ontology (GO) terms are response to chitin, defense response incompatible interaction, response to organonitrogen compound, defense response to bacteria, and response to fungus (Fig. 3D).

SA is an important phytohormone that mediates plant immunity. Large amounts of SA are often accumulated in autoimmune plants (Zhang *et al.*, 2003; Chakraborty *et al.*, 2018). We measured SA concentrations in *RIN13* and Col-0 plants, and the SA concentration in *RIN13* plants increased 4-fold relative to that in Col-0 (Fig. 3E). The elevated mRNA levels of SA synthesis-related genes (*ICS1* and *EDS5*) and the downstream signaling genes (*NPR1*, *PR1*, and *PR2*) in *RIN13* plants further substantiate the conclusion that RIN13 stimulates SA synthesis and SA signaling (Fig. 3F). These results, together with the dwarfism phenotype of *RIN13* plants in Fig. 1, clearly indicated that overexpression of *RIN13* induces autoimmunity.

SA-dependent and SA-independent pathways are both required for RIN13 to promote disease resistance

We genetically dissected the effects of SA and SA signaling on the function of RIN13. *RIN13* plants were crossed with *sid2-2*,

an SA synthesis-defective mutant (Yang *et al.*, 2015; Rekhter *et al.*, 2019), and *npr1-1*, an SA signaling-defective mutant (Cao *et al.*, 1997), respectively. Introduction of either mutant could not restore the dwarf phenotype triggered by RIN13 (Fig. 4A; Supplementary Fig. S4A), and the protein levels of RIN13 were not affected by either *sid2-2* or *npr1-1* (Fig. 4B; Supplementary Fig. S4B). The accumulation of SA and constitutive expression of *PR1*, a classic marker gene for SA activation, were markedly repressed in *sid2-2* as well as in *RIN13 sid2-2*, indicating that SA-mediated signaling was blocked by *sid2-2* (Fig. 4C, D). Other disease resistance-related genes we examined, including *PAD4*, *EDS1*, *ADR1*, *FMO1*, and *ALD1* (Dong *et al.*, 2016; Hartmann *et al.*, 2018), were all up-regulated in *RIN13 sid2-2* in comparison with those in *sid2-2*, indicating that RIN13 could impact some defense-related genes independent of SA (Fig. 4E–I). However, as shown in Fig. 4J, *RIN13 sid2-2* plants displayed a significant ($P < 0.001$) reduction in disease resistance relative to *RIN13* plants, suggesting that SA and SA signaling are required for RIN13-mediated disease resistance. Nonetheless, *RIN13 sid2-2* plants still displayed higher disease resistance than *sid2-2* plants, implying that RIN13 can mediate some disease resistance independently of SA (Fig. 4J). Taken together, these results suggest that RIN13 requires both SA-dependent and SA-independent pathways to enhance disease resistance.

The EDS1/PAD4 complex mediates RIN13-induced dwarfism and disease resistance

PAD4 functions upstream of SA, and mediates both SA-dependent and SA-independent immune pathways (Zhou *et al.*, 1998). To examine whether PAD4 mediates the function

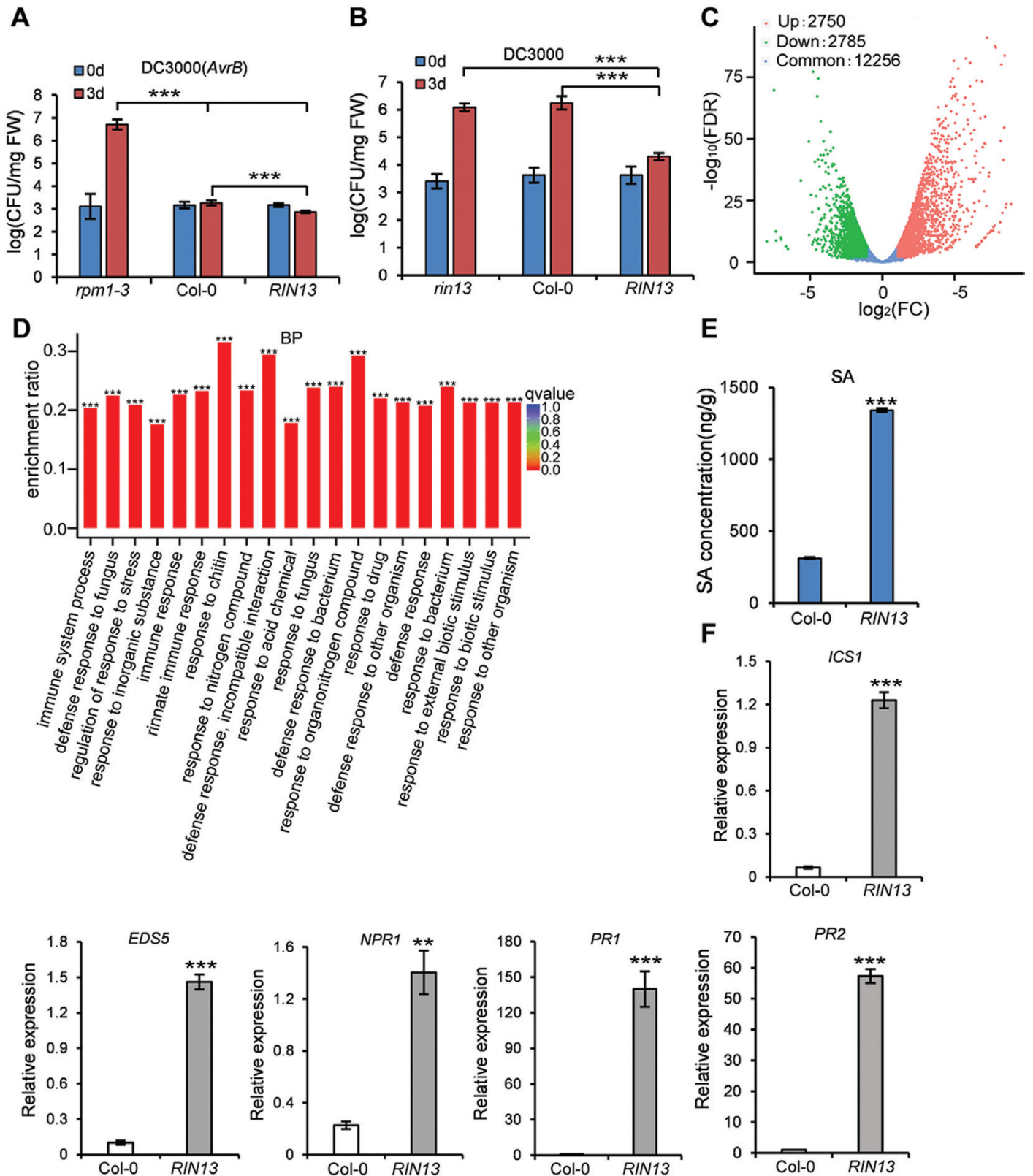


Fig. 3. Overexpression of *RIN13* activates the plant immune response. (A) *RIN13* plants show stronger resistance to *P. syringae* pathovar *tomato* (*Pst*) DC3000 (*AvrB*) than the wild-type plants. Four-week-old plants were spray-inoculated with 2.5×10^7 CFU ml⁻¹ of a bacterial suspension. Growth of bacteria was assessed at 0 d and 3 d post-inoculation, respectively. The *RPM1* loss-of-function mutant *rpm1-3* was used as a negative control for *Pst* DC3000 (*AvrB*). (B) *RIN13* plants show stronger resistance to *Pst* DC3000 than the wild-type plants and *rin13* mutant. (C) Volcano plot of DEGs in *RIN13* compared with those in Col-0. The leaves from 4-week-old *RIN13* and Col-0 plants grown under a 16 h/8 h light/dark cycle were used for RNA-seq analysis. The 2750 up-regulated genes and 2785 down-regulated genes were selected with log₂ (FC) > 1, or log₂ (FC) < -1. A false discovery rate (FDR) < 0.05 was used to determine the significance of DEGs. (D) Gene Ontology (GO) enrichments of the up-regulated genes. BP: biological process. Significantly enriched GO terms are marked with *** ($q < 0.001$). (E) SA concentrations in *RIN13* and Col-0 plants. Leaves from 50 six-week-old plants

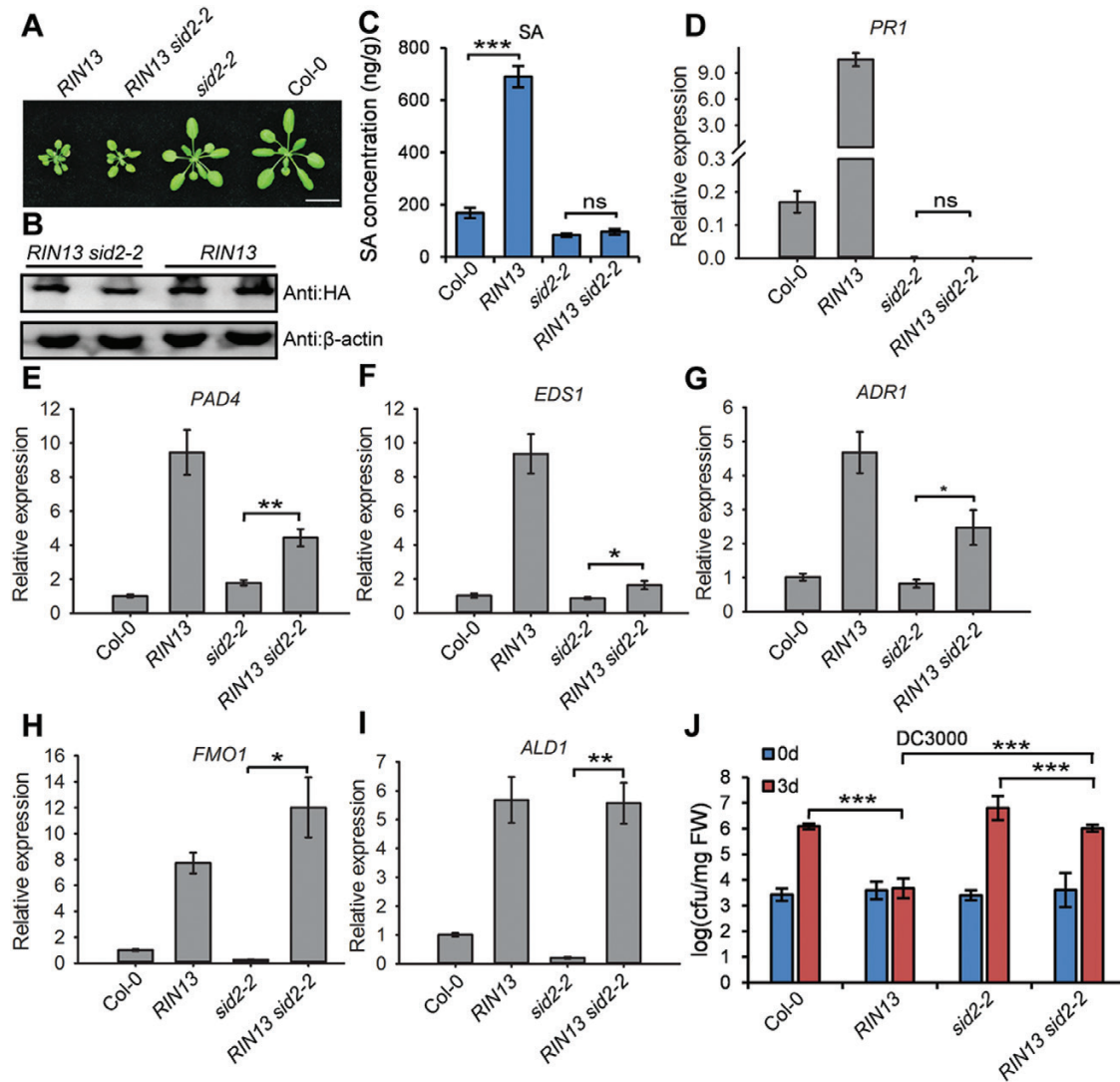


Fig. 4. Effects of SA and SA signaling on RIN13-induced disease resistance. (A) *sid2-2* did not restore the dwarf phenotype induced by RIN13. RIN13 plants were crossed with *sid2-2*, a loss-of-function mutant for SA synthesis. Four-week-old plants grown under a 16 h/8 h light/dark cycle were photographed. Scale bar=2 cm. (B) The protein level of RIN13 in plants. RIN13–YFP–HA was detected with an anti-HA antibody in RIN13 *sid2-2* and RIN13 plants. (C) SA concentrations in Col-0, RIN13, *sid2-2*, and RIN13 *sid2-2* plants. Four-week-old plants were used to measure the concentrations of SA. (D–I) The transcriptional levels of disease resistance-related genes in plants. Four-week-old plants were used to extract RNA for subsequent qRT–PCR. The relative expression was detected by qRT–PCR using *ACTIN 2* as the internal control. Results are means \pm SE of three biological repeats. Significant differences were measured by Student's *t*-test, and marked as ** $P < 0.01$ and * $P < 0.05$. A non-significant difference was marked as ns. (J) RIN13 induced both SA-dependent and SA-independent immunity. Four-week-old plants grown under an 8 h/16 h light/dark cycle were spray-inoculated with *Pst* DC3000 (2.5×10^7 CFU ml $^{-1}$). Values are means \pm SD of four biological replicates. Significant differences were measured by Student's *t*-test and marked as *** $P < 0.001$. *ADR1*, Activated disease resistance 1; *ALD1*, AGD2-like defense response protein 1; *FMO1*, Flavin containing dimethylaniline monooxygenase 1; *SID2*, Salicylic acid induction deficient 2 (or Isochorismate synthase 1). (This figure is available in color at JXB online.)

of RIN13, we crossed RIN13 plants with *pad4-1* (Jirage *et al.*, 1999). Our results showed that the *pad4-1* mutant completely restored the dwarf phenotype of RIN13 (Fig. 5A). Since the protein level of RIN13 in RIN13 *pad4-1* was similar to that in RIN13 plants, the phenotype restored by mutant *pad4-1* is not due to the decrease of RIN13 protein level (Fig. 5B). Then, we measured the SA concentrations, and our results showed

that the increased SA concentration in RIN13 plants was compromised by PAD4 deficiency (Fig. 5C). Consistently, the expression of disease-related genes including *PR1*, *EDS1*, *ADR1*, *FMO1*, and *ALD1* was greatly repressed in RIN13 *pad4-1* plants compared with RIN13 plants (Fig. 5D–H). RIN13 lost the ability to up-regulate the expression of genes such as *EDS1*, *ADR1*, *FMO1*, and *ALD1* in the *pad4-1* background

were pooled to measure the concentrations of SA. (F) Quantitative analysis of SA synthesis-related genes (*ICS1* and *EDS5*) and signaling genes (*NPR1*, *PR1*, and *PR2*) by qRT–PCR. Results are means \pm SE of three biological repeats. *ACTIN 2* was used as an internal control. Significant differences were measured by Student's *t*-test and marked as *** $P < 0.001$ and ** $P < 0.01$. DEGs, differentially expressed genes; FC, fold change. (This figure is available in color at JXB online.)

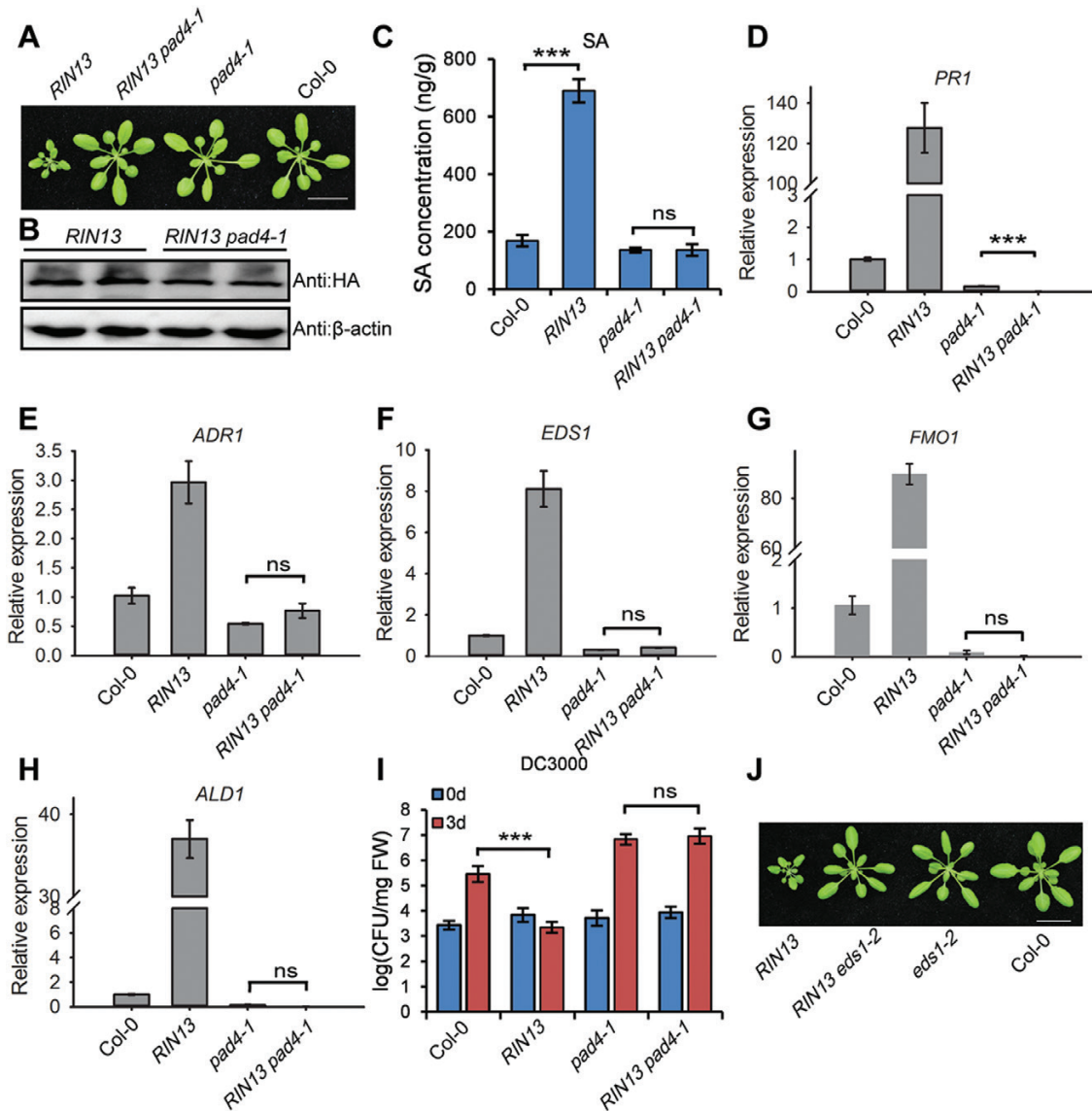


Fig. 5. EDS1/PAD4 mediates the function of RIN13. (A) *pad4-1* rescued the dwarf phenotype of *RIN13* plants. *RIN13* plants were crossed with *pad4-1*. Four-week-old plants grown under a 16 h/8 h light/dark cycle were photographed. Scale bar=2 cm. (B) The protein level of RIN13 in plants. (C) SA concentrations in Col-0, *RIN13*, *pad4-1*, and *RIN13 pad4-1* plants. Four-week-old plants were used to measure the concentrations of SA. (D–H) The transcriptional level of disease resistance-related genes in plants. The relative expression was detected by qRT-PCR using *ACTIN 2* as the internal control. Results are means \pm SE of three biological repeats. Significant differences were measured by Student's *t*-test, and marked as ****P*<0.001. (I) The *RIN13*-mediated disease resistance to *Pst* DC3000 was abolished in *RIN13 pad4-1* plants. Four-week-old plants grown under an 8/16 h light/dark cycle were spray-inoculated with *Pst* DC3000 (2.5×10^7 CFU ml⁻¹). Values are means \pm SD of four biological replicates. Significant differences were measured by Student's *t*-test, and marked as ****P*<0.001. (J) The deficiency of *EDS1* rescued the *RIN13*-mediated dwarf phenotype. Four-week-old plants grown under a 16 h/8 h light/dark cycle were photographed. Scale bar=2 cm. ns, non-significant difference. (This figure is available in color at JXB online.)

whereas it effectively induced the expression of these genes in the *sid2-2* mutant. *RIN13 pad4-1* plants were equally susceptible to *Pst* DC3000 as *pad4-1* (Fig. 5I), indicating that *RIN13*-mediated resistance is completely abolished in the *pad4-1* mutant. Therefore, we concluded that the function of *RIN13* is dependent upon *PAD4*.

PAD4 usually functions with *EDS1* as a complex, thus we further investigated whether *RIN13* plays its role with *EDS1*. We generated *RIN13 eds1-2* plants by crossing *RIN13* plants with *eds1-2* (Falk *et al.*, 1999). Our results showed that the dwarf phenotype of *RIN13* plants was completely abolished in *RIN13 eds1-2* plants (Fig. 5J), suggesting that both *EDS1* and *PAD4* mediate the *RIN13*-induced dwarf phenotype.

RIN13 increases the accumulation of *PAD4* in the nucleus

To interrogate the association between *EDS1/PAD4* and *RIN13* at the protein level, T7-*RIN13* was transiently co-expressed with *PAD4-YFP-HA* or *EDS1-YFP-HA* in *N. benthamiana* to determine whether *RIN13* affects the protein levels of *PAD4-YFP-HA* and *EDS1-YFP-HA* or their distributions between the nucleus and cytoplasm. Our results showed that *RIN13* did not affect the protein levels of *EDS1-YFP-HA* and *PAD4-YFP-HA*, but noticeably changed the subcellular distribution of *PAD4* (Fig. 6A, B). We also quantified the fluorescence intensities of >30 nuclei in

N. benthamiana leaves expressing PAD4-YFP-HA with and without T7-RIN13, respectively, and found that co-expression with RIN13 greatly elevated the intensity of PAD4-YFP-HA in the nuclei (Fig. 6C), indicating that RIN13 promotes the nuclear accumulation of PAD4. Consistent with the confocal data, cytoplasmic-nuclear fractionation assays showed nuclear enrichment of PAD4-YFP-HA in the presence of RIN13 (Fig. 6D). To our surprise, RIN13 does not affect the distribution patterns of EDS1-YFP-HA in either the cytoplasm or the nucleus (Fig. 6B-D).

The dwarf phenotype of RIN13 is temperature sensitive, and partially depends on SNC1

As described above, *RIN13* plants are severely dwarfed when grown at 22 °C. However, when 2-week-old *RIN13* plant seedlings were transferred to, and grown under 28 °C for another 2 weeks, the phenotypic defects of *RIN13* largely disappeared (Fig. 7A), suggesting that a high growth temperature could rescue the dwarf phenotype induced by *RIN13* overexpression. The high temperature did not affect the

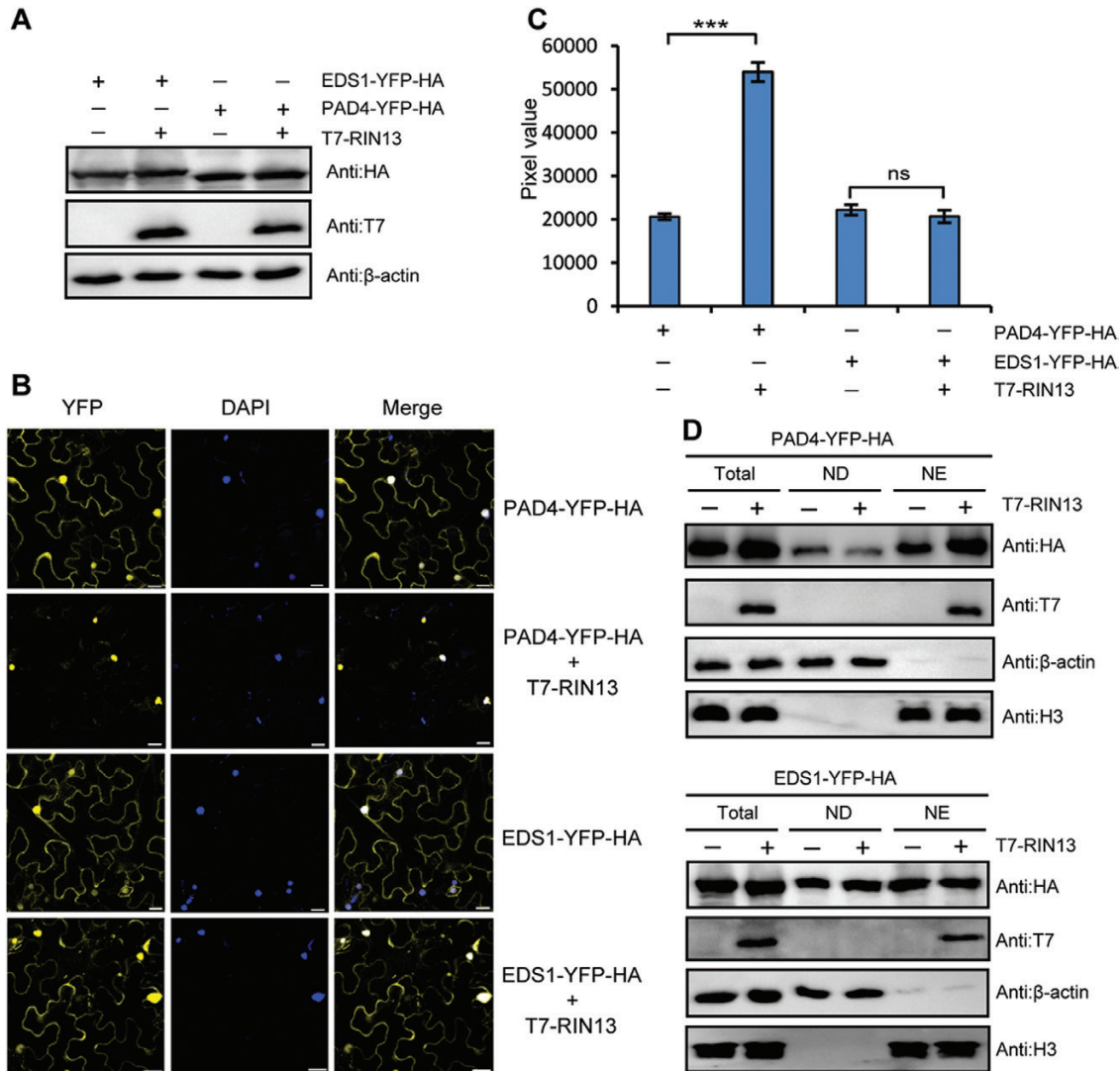


Fig. 6. RIN13 increases the accumulation of PAD4 in the nucleus. (A) RIN13 did not affect the protein level of EDS1-YFP-HA or PAD4-YFP-HA. *35S::EDS1-YFP-HA* or *35S::PAD4-YFP-HA* were transiently expressed in the leaves of *N. benthamiana* with or without *35S::T7-RIN13*. The protein level of EDS1-YFP-HA or PAD4-YFP-HA was detected with an anti-HA antibody, and the protein level of T7-RIN13 was detected with an anti-T7 antibody. β-Actin was used as an internal loading control. (B) The subcellular localization of PAD4-YFP-HA or EDS1-YFP-HA in *N. benthamiana*. Agrobacteria containing the *35S::PAD4-YFP-HA* or *35S::EDS1-YFP-HA* expression construct ($OD_{600}=0.3$) were co-infiltrated with or without agrobacteria containing the *35S::T7-RIN13* expression construct ($OD_{600}=0.5$) in the leaves of *N. benthamiana*. The distribution of PAD4-YFP-HA or EDS1-YFP-HA was observed with confocal microscopy at 2 d post-infiltration. Nuclei were stained with DAPI. Scale bar=20 μm. (C) Quantitative analysis of the fluorescence intensity in nuclei. The fluorescence images were collected at identical settings. The fluorescence intensity in the nucleus was quantified. Results are means \pm SE of >30 nuclei. Significant differences were measured by Student's *t*-test, and marked as *** $P<0.001$. No significant difference was marked as ns. (D) Fractionation assays of PAD4-YFP-HA and EDS1-YFP-HA with/without T7-RIN13. Total proteins (Total) from transiently expressed *N. benthamiana* leaves were separated into the nuclear-depleted fraction (ND) and nuclear-enriched fraction (NE). β-Actin and histone H3 were used as internal references for ND and NE proteins, respectively. (This figure is available in color at JXB online.)

protein level of RIN13 (Fig. 7B). Since the EDS1/PAD4 complex mediates the function of RIN13 as well as the function of TNL proteins, the fact that *snc1-1*, a gain-of-function mutant of *SNC1* which encodes a classic TNL protein, exhibits constitutive defense responses and a dwarf phenotype at 22 °C but not at 28 °C (Zhu *et al.*, 2010), prompted us to further explore whether the exemplary TNL protein *SNC1* mediates the function of RIN13. To this end, we crossed *RIN13* plants with *snc1-r1*, a loss-of-function mutant of *SNC1* (Zhang *et al.*, 2003), to generate *RIN13 snc1-r1* plants. Our results showed that *snc1-r1* partially but clearly restored the dwarf phenotype of *RIN13* plants, suggesting that TNL proteins are required for the function of RIN13 (Fig. 7C, D).

Discussion

In a previous report by Al-Daoude *et al.* (2005), the authors produced no evidence that overexpression of *RIN13* could cause morphological defects. However, in this study, we observed that *35S::RIN13-YFP-HA* transgenic plants displayed a clear dwarfism. The discrepancy is probably due to the variations in RIN13 expression levels, as the severity of the dwarf phenotype was tightly correlated with RIN13 protein levels (Fig. 1A, B). It has long been appreciated that silencing or variable transgene expression levels occurred frequently, particularly when the transgene was under the control of strong, constitutive promoters, such as CaMV 35S (De Buck *et al.*, 2013). The transgenic plant (line #9) used in our study has a very high abundance of RIN13 protein, whereas the lines used by Al-Daoude *et al.* (2005) showed quite a low expression of RIN13. Also, Al Daoude *et al.* (2005) reported that RIN13 does not enhance resistance to *Pst* DC3000, while we showed

that RIN13 confers plants with strong resistance. Besides variations in the RIN13 expression levels, another very possible explanation for this discrepancy is the different experimental methods used in the two studies. We inoculate the pathogens by spray, whereas Al Daoude *et al.* (2005) used a syringe infiltration inoculation method. However, our results showing that overexpression of *RIN13* enhances disease resistance are consistent with the previous report.

Although RIN13 positively regulates the function of the CNL protein RPM1, *rpm1-3* did not suppress the RIN13-induced phenotype, indicating that RIN13 can induce plant immunity independently of RPM1 (Fig. 1G). The mutant *snc1-r1* suppressed the RIN13-induced phenotype. Overexpression of *RIN13* may directly or indirectly lead to the high accumulation of TNL proteins (including *SNC1*) or the activation of TNL proteins. There are two clues to further explore the function of RIN13. The first clue is that RIN13 was originally found to interact with the NB-ARC domain of RPM1 which is highly conserved in both CNL and TNL proteins (Al-Daoude *et al.*, 2005); it is possible that RIN13 can interact with some TNL proteins to affect their function. The second clue is that RIN13 may function as a transcriptional mediator to affect gene expression based on the fact that RIN13 functions in the nucleus. In addition, RIN13 was autoactivated in a yeast two-hybrid (Y2H) system when it was fused with the Gal4 DNA-binding domain (BD), suggesting that RIN13 can affect gene expression (Supplementary Fig. S5). RIN13 is composed of 430 amino acids without any verified domains. Identification of the RIN13-interacting proteins, especially those in the nucleus, will help to explain the correlation between RIN13 and TNL proteins.

RIN13 is a nuclear-localized protein. When co-expressed with PAD4, RIN13 can drive PAD4 into the nucleus (Fig. 6). PAD4 mediates both RIN13-induced phenotypes and RIN13-enhanced disease resistance (Fig. 5A, I). These results could be perfectly explained if RIN13 interacted with PAD4, but, up to now, no interaction between RIN13 and PAD4 was detected with Y2H or bimolecular fluorescence complementation (BiFC) assays. We have tried but failed to conduct co-immunoprecipitation (Co-IP) experiments because of the difficulty in extracting RIN13 protein in a soluble state. Thus, we could not rule out the possibility that RIN13 affects the nuclear location of PAD4 indirectly.

Although it is well known that EDS1 and PAD4 shuttle between the cytoplasm and nucleus, the underlying mechanism remains obscure so far. Our results showing that RIN13 could drive PAD4 into the nucleus in transient expression experiments using *N. benthamiana* leaves (Fig. 6) may shed some light on the regulatory mechanism of changes for the subcellular localization of PAD4 in plants. We also observed that RIN13 could increase the accumulation of PAD4, but not EDS1, in the nucleus in *N. benthamiana* leaves (Fig. 6). This may be explained by the fact that the transiently expressed EDS1 from *Arabidopsis* cannot pair well with PAD4 from *N. benthamiana* based on the fact that EDS1 and PAD4 co-evolved within species, and they do not pair well from different species (Lapin *et al.*, 2019).

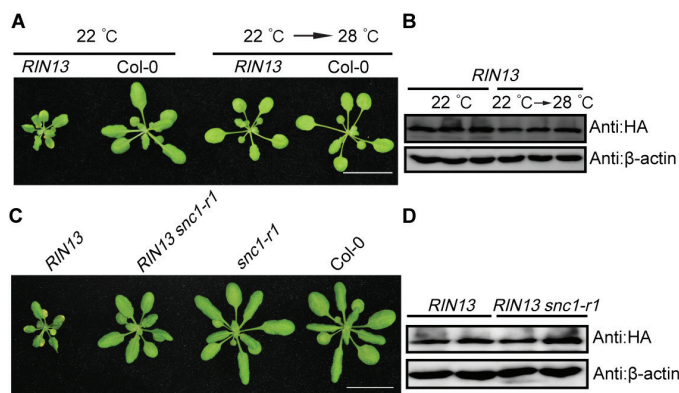


Fig. 7. High temperature rescues the dwarf phenotype of *RIN13*. (A) Phenotypes of *RIN13* and *Col-0* plants under different temperatures. Plants were grown under two different conditions; 22 °C indicates that plants were grown at 22 °C for 4 weeks; 22 °C → 28 °C indicates that 2-week-old plants grown at 22 °C were transferred to 28 °C for another 2 weeks. Scale bar=2 cm. (B) The protein level of RIN13 was not affected by temperature. (C) *snc1-r1* partially rescued the dwarf phenotype of *RIN13*. *RIN13* plants were crossed with *snc1-r1*, a loss-of-function mutant of *SNC1*. Four-week-old plants grown under a 16/8 h light/dark cycle at 22 °C were used to show the morphological difference. Scale bar=2 cm. (D) *snc1-r1* mutation did not affect the protein level of RIN13. *SNC1*, *Suppressor of npr1-1, constitutive 1*. (This figure is available in color at JXB online.)

Our genetic analysis indicates that SNC1 and EDS1/PAD4 mediate RIN13-induced disease resistance. Based on the fact that the EDS1/PAD4 protein complex functions downstream of TNL proteins to mediate their resistance (Wiermer *et al.*, 2005), we speculated that EDS1/PAD4 acts downstream of TNL proteins (with SNC1 as representative). Both *RIN13* and *RIN13 sid2-2* plants have the dwarf phenotypes, but *RIN13* plants showed much stronger defense responses, suggesting that SA and SA signaling are required for RIN13-mediated resistance (Fig. 4). However, *RIN13 sid2-2* still had stronger resistance than *sid2-2*, suggesting that RIN13 can also partially enhance the disease resistance independently of SA (Fig. 4J). In addition, the *eds1-2* or *pad4-1* mutant totally restored the dwarf phenotype induced by RIN13, revealing that the EDS1/PAD4 complex is a critical integration point to control RIN13-induced signal output (Figs 5, 8). Together, our study uncovered a signaling pathway whereby SNC1 and EDS1/PAD4 act together to modulate RIN13-triggered plant immunity (Fig. 8).

This study clearly demonstrates that overexpression of RIN13 induces TNL-mediated autoimmunity. RIN13 may affect the protein level of TNLs or change their subcellular locations to stimulate the activity of TNLs. RIN13 is possibly directly guarded by one or more TNLs, and its overexpression could lead to the activation of the proteins. Likewise, overexpression of RIN13 might indirectly activate TNLs by modifying targets guarded by the TNLs. The

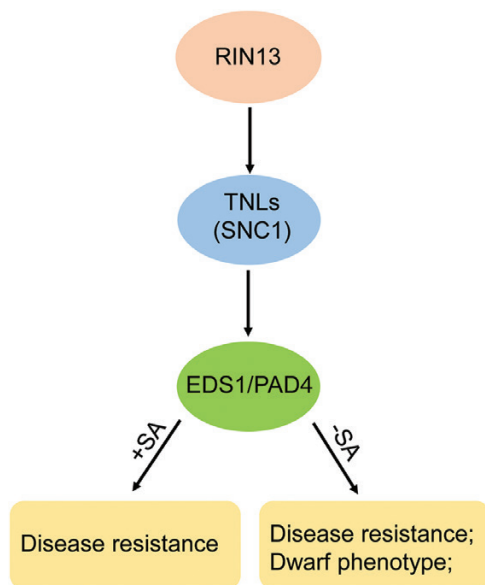


Fig. 8. A schematic signal transduction pathway of RIN13. We put RIN13 upstream of TNLs, such as SNC1, due to the compromised phenotype of *RIN13* in the *snc1-r1* mutant. The resistance of TNL proteins depends on the EDS1/PAD4 complex which usually acts as a central node to regulate downstream defense signals. The defense signals of EDS1/PAD4 can be divided into two categories: SA dependent and SA independent. SA and SA signaling contribute to RIN13-mediated disease resistance. However, RIN13-induced dwarf phenotype and partial disease resistance are SA independent, but EDS1/PAD4 dependent. TNLs, Toll-like/Interleukin 1 receptor (TIR) nucleotide-binding (NB) leucine-rich repeats (LRR); SNC1, Suppressor of *npr1-1*, constitutive 1; EDS1, Enhanced disease susceptibility 1; PAD4: Phytoalexin deficient 4; SA, salicylic acid. (This figure is available in color at *JXB* online.)

mechanism by which RIN13 stimulates the activity of TNLs merits further investigation.

Supplementary data

The following supplementary data are available at *JXB* online.

Fig. S1. The developmental phenotypes of *RIN13* transgenic plants.

Fig. S2. RIN13 functions in the nucleus.

Fig. S3. *RIN13-L* may phenocopy *RIN13*.

Fig. S4. The *npr1-1* mutation does not rescue the RIN13-induced dwarf phenotype.

Fig. S5. RIN13-BD but not RIN13-AD is autoactive in the yeast two-hybrid system.

Table S1. Primers used to identify the Arabidopsis mutants in this study.

Table S2. qRT-PCR primers used in this study.

Acknowledgements

We would like to thank Dr Jeffery L. Dangl (University of North Carolina at Chapel Hill), Dr Wei Xiao (University of Saskatchewan), Dr Xin Li (University of British Columbia), Dr Haitao Cui (Fujian Agriculture and Forestry University), Dr Ying-Tang Lu (Wuhan University), and Dr Guoyong Xu (Wuhan University) for providing plant seeds. We also thank Dr Murray Grant, Dr Li Wan, Dr N uria S anchez Coll, and Dr Marc T. Nishimura for critical reading. This work was funded by The National Key Research and Development Program of China (2016YFD0100600) and the National Natural Science Foundation of China under grant numbers 31270315 and 31770282.

Author contributions

ZG and XL planned and designed the research. XL, HL, JH, SZ, HH, and ZW performed the experiments. ZG, XL, Y-KL, and W-CL analyzed the data and wrote the manuscript. All authors read and approved the manuscript.

Data availability

The raw data of RNA-seq described in this study have been deposited in the NCBI database under accession number PRJNA631584.

References

- Al-Daoude A, de Torres Zabala M, Ko JH, Grant M. 2005. RIN13 is a positive regulator of the plant disease resistance protein RPM1. *The Plant Cell* **17**, 1016–1028.
- Cao H, Glazebrook J, Clarke JD, Volko S, Dong X. 1997. The *Arabidopsis NPR1* gene that controls systemic acquired resistance encodes a novel protein containing ankyrin repeats. *Cell* **88**, 57–63.
- Chakraborty J, Ghosh P, Das S. 2018. Autoimmunity in plants. *Planta* **248**, 751–767.
- Chen H, Xue L, Chintamanani S, *et al.* 2009. ETHYLENE INSENSITIVE3 and ETHYLENE INSENSITIVE3-LIKE1 repress SALICYLIC ACID INDUCTION DEFICIENT2 expression to negatively regulate plant innate immunity in *Arabidopsis*. *The Plant Cell* **21**, 2527–2540.
- Clough SJ, Bent AF. 1998. Floral dip: a simplified method for *Agrobacterium*-mediated transformation of *Arabidopsis thaliana*. *The Plant Journal* **16**, 735–743.

- Couto D, Zipfel C.** 2016. Regulation of pattern recognition receptor signalling in plants. *Nature Reviews. Immunology* **16**, 537–552.
- Cui H, Gobbato E, Kracher B, Qiu J, Bautor J, Parker JE.** 2017. A core function of EDS1 with PAD4 is to protect the salicylic acid defense sector in *Arabidopsis* immunity. *New Phytologist* **213**, 1802–1817.
- Cui H, Qiu J, Zhou Y, Bhandari DD, Zhao C, Bautor J, Parker JE.** 2018. Antagonism of transcription factor MYC2 by EDS1/PAD4 complexes bolsters salicylic acid defense in *Arabidopsis* effector-triggered immunity. *Molecular Plant* **11**, 1053–1066.
- Cui H, Tsuda K, Parker JE.** 2015. Effector-triggered immunity: from pathogen perception to robust defense. *Annual Review of Plant Biology* **66**, 487–511.
- De Buck S, De Paepe A, Depicker A.** 2013. Transgene expression in plants, control of. In: Christou P, Savin R, Costa-Pierce BA, Misztal I, Whitelaw CBA, eds. *Sustainable food production*. New York: Springer New York, 1570–1593.
- Ding B, Bellizzi Mdel R, Ning Y, Meyers BC, Wang GL.** 2012. HDT701, a histone H4 deacetylase, negatively regulates plant innate immunity by modulating histone H4 acetylation of defense-related genes in rice. *The Plant Cell* **24**, 3783–3794.
- Ding Y, Sun T, Ao K, Peng Y, Zhang Y, Li X, Zhang Y.** 2018. Opposite roles of salicylic acid receptors NPR1 and NPR3/NPR4 in transcriptional regulation of plant immunity. *Cell* **173**, 1454–1467.e15.
- Dobrev PI, Vankova R.** 2012. Quantification of abscisic acid, cytokinin, and auxin content in salt-stressed plant tissues. *Methods in Molecular Biology* **913**, 251–261.
- Dodds PN, Rathjen JP.** 2010. Plant immunity: towards an integrated view of plant–pathogen interactions. *Nature Reviews. Genetics* **11**, 539–548.
- Dong OX, Tong M, Bonardi V, El Kasmi F, Woloshen V, Wunsch LK, Dangl JL, Li X.** 2016. TNL-mediated immunity in *Arabidopsis* requires complex regulation of the redundant ADR1 gene family. *New Phytologist* **210**, 960–973.
- Dongus JA, Bhandari DD, Patel M, Archer L, Dijkgraaf L, Deslandes L, Shah J, Parker JE.** 2020. The *Arabidopsis* PAD4 lipase-like domain is sufficient for resistance to green peach aphid. *Molecular Plant-Microbe Interactions* **33**, 328–335.
- Falk A, Feys BJ, Frost LN, Jones JD, Daniels MJ, Parker JE.** 1999. EDS1, an essential component of *R* gene-mediated disease resistance in *Arabidopsis* has homology to eukaryotic lipases. *Proceedings of the National Academy of Sciences, USA* **96**, 3292–3297.
- Feys BJ, Moisan LJ, Newman MA, Parker JE.** 2001. Direct interaction between the *Arabidopsis* disease resistance signaling proteins, EDS1 and PAD4. *The EMBO Journal* **20**, 5400–5411.
- Fu ZQ, Dong X.** 2013. Systemic acquired resistance: turning local infection into global defense. *Annual Review of Plant Biology* **64**, 839–863.
- Fu ZQ, Yan S, Saleh A, et al.** 2012. NPR3 and NPR4 are receptors for the immune signal salicylic acid in plants. *Nature* **486**, 228–232.
- Gaffney T, Friedrich L, Vernooij B, Negrotto D, Nye G, Uknes S, Ward E, Kessmann H, Ryals J.** 1993. Requirement of salicylic acid for the induction of systemic acquired resistance. *Science* **261**, 754–756.
- Gao Z, Gao Z, Chung EH, Eitas TK, Dangl JL.** 2011. Plant intracellular innate immune receptor Resistance to *Pseudomonas syringae* *pv. maculicola* 1 (RPM1) is activated at, and functions on, the plasma membrane. *Proceedings of the National Academy of Sciences, USA* **108**, 7619–7624.
- Grant MR, Godiard L, Straube E, Ashfield T, Lewald J, Sattler A, Innes RW, Dangl JL.** 1995. Structure of the *Arabidopsis* *RPM1* gene enabling dual specificity disease resistance. *Science* **269**, 843–846.
- Hartmann M, Zeier T, Bernsdorff F, et al.** 2018. Flavin monooxygenase-generated N-hydroxypipicolinic acid is a critical element of plant systemic immunity. *Cell* **173**, 456–469.e16.
- Jirage D, Tootle TL, Reuber TL, Frost LN, Feys BJ, Parker JE, Ausubel FM, Glazebrook J.** 1999. *Arabidopsis thaliana* PAD4 encodes a lipase-like gene that is important for salicylic acid signaling. *Proceedings of the National Academy of Sciences, USA* **96**, 13583–13588.
- Jones JD, Dangl JL.** 2006. The plant immune system. *Nature* **444**, 323–329.
- Jones JD, Vance RE, Dangl JL.** 2016. Intracellular innate immune surveillance devices in plants and animals. *Science* **354**, aaf6395.
- Karimi M, Inzé D, Depicker A.** 2002. GATEWAY vectors for *Agrobacterium*-mediated plant transformation. *Trends in Plant Science* **7**, 193–195.
- Kim D, Langmead B, Salzberg SL.** 2015. HISAT: a fast spliced aligner with low memory requirements. *Nature Methods* **12**, 357–360.
- Kinkema M, Fan W, Dong X.** 2000. Nuclear localization of NPR1 is required for activation of PR gene expression. *The Plant Cell* **12**, 2339–2350.
- Lapin D, Kovacova V, Sun X, et al.** 2019. A coevolved EDS1–SAG101–NRG1 module mediates cell death signaling by TIR-domain immune receptors. *The Plant Cell* **31**, 2430–2455.
- Li Z, Huang J, Wang Z, Meng F, Zhang S, Wu X, Zhang Z, Gao Z.** 2019. Overexpression of *Arabidopsis* nucleotide-binding and leucine-rich repeat genes *RPS2* and *RPM1(D505V)* confers broad-spectrum disease resistance in rice. *Frontiers in Plant Science* **10**, 417.
- Liu X, Liu H, Liu WC, Gao Z.** 2020. The nuclear localized RIN13 induces cell death through interacting with ARF1. *Biochemical and Biophysical Research Communications* **527**, 124–130.
- Pegadaraju V, Louis J, Singh V, Reese JC, Bautor J, Feys BJ, Cook G, Parker JE, Shah J.** 2007. Phloem-based resistance to green peach aphid is controlled by *Arabidopsis* PHYTOALEXIN DEFICIENT4 without its signaling partner ENHANCED DISEASE SUSCEPTIBILITY1. *The Plant Journal* **52**, 332–341.
- Rekhter D, Lüdke D, Ding Y, Feussner K, Zienkiewicz K, Lipka V, Wiermer M, Zhang Y, Feussner I.** 2019. Isochorismate-derived biosynthesis of the plant stress hormone salicylic acid. *Science* **365**, 498–502.
- Robinson MD, McCarthy DJ, Smyth GK.** 2010. edgeR: a Bioconductor package for differential expression analysis of digital gene expression data. *Bioinformatics* **26**, 139–140.
- Shirano Y, Kachroo P, Shah J, Klessig DF.** 2002. A gain-of-function mutation in an *Arabidopsis* Toll Interleukin1 receptor-nucleotide binding site-leucine-rich repeat type R gene triggers defense responses and results in enhanced disease resistance. *The Plant Cell* **14**, 3149–3162.
- Tang D, Wang G, Zhou JM.** 2017. Receptor kinases in plant–pathogen interactions: more than pattern recognition. *The Plant Cell* **29**, 618–637.
- Tornero P, Dangl JL.** 2001. A high-throughput method for quantifying growth of phytopathogenic bacteria in *Arabidopsis thaliana*. *The Plant Journal* **28**, 475–481.
- Uknes S, Mauch-Mani B, Moyer M, Potter S, Williams S, Dincher S, Chandler D, Slusarenko A, Ward E, Ryals J.** 1992. Acquired resistance in *Arabidopsis*. *The Plant Cell* **4**, 645–656.
- Vlot AC, Dempsey DA, Klessig DF.** 2009. Salicylic acid, a multifaceted hormone to combat disease. *Annual Review of Phytopathology* **47**, 177–206.
- Wagner S, Stuttmann J, Rietz S, Guerois R, Brunstein E, Bautor J, Niefind K, Parker JE.** 2013. Structural basis for signaling by exclusive EDS1 heteromeric complexes with SAG101 or PAD4 in plant innate immunity. *Cell Host & Microbe* **14**, 619–630.
- Wiermer M, Feys BJ, Parker JE.** 2005. Plant immunity: the EDS1 regulatory node. *Current Opinion in Plant Biology* **8**, 383–389.
- Wildermuth MC, Dewdney J, Wu G, Ausubel FM.** 2001. Isochorismate synthase is required to synthesize salicylic acid for plant defence. *Nature* **414**, 562–565.
- Wirthmueller L, Zhang Y, Jones JD, Parker JE.** 2007. Nuclear accumulation of the *Arabidopsis* immune receptor RPS4 is necessary for triggering EDS1-dependent defense. *Current Biology* **17**, 2023–2029.
- Yang L, Li B, Zheng XY, Li J, Yang M, Dong X, He G, An C, Deng XW.** 2015. Salicylic acid biosynthesis is enhanced and contributes to increased biotrophic pathogen resistance in *Arabidopsis* hybrids. *Nature Communications* **6**, 7309.
- Yuan HM, Liu WC, Lu YT.** 2017. CATALASE2 coordinates SA-mediated repression of both auxin accumulation and JA biosynthesis in plant defenses. *Cell Host & Microbe* **21**, 143–155.
- Yuan X, Wang Z, Huang J, Xuan H, Gao Z.** 2018. Phospholipidase Dδ negatively regulates the function of resistance to *Pseudomonas syringae* *pv. Maculicola* 1 (RPM1). *Frontiers in Plant Science* **9**, 1991.
- Zhang Y, Goritschnig S, Dong X, Li X.** 2003. A gain-of-function mutation in a plant disease resistance gene leads to constitutive activation of downstream signal transduction pathways in *suppressor of npr1-1, constitutive 1*. *The Plant Cell* **15**, 2636–2646.
- Zhou N, Tootle TL, Tsui F, Klessig DF, Glazebrook J.** 1998. PAD4 functions upstream from salicylic acid to control defense responses in *Arabidopsis*. *The Plant Cell* **10**, 1021–1030.
- Zhu Y, Qian W, Hua J.** 2010. Temperature modulates plant defense responses through NB-LRR proteins. *PLoS Pathogens* **6**, e1000844.